OpenXstim: an open-source programmable electrical stimulator for transcutaneous spinal cord stimulation therapy

Journal of Neural Engineering

PAPER

OPEN ACCESS

RECEIVED
22 September 2025

REVISED
2 November 2025

ACCEPTED FOR PUBLICATION
18 November 2025

PUBLISHED
27 November 2025

OpenXstim: an open-source programmable electrical stimulator for transcutaneous spinal cord stimulation therapy

Monzurul Alam[1,2,*], **Vaheh Nazari**[3], **Md Akhlasur Rahman**[4], **Vijayapriya Arumugam**[5], **Naveena Narayanan**[5], **Farjana Taoheed**[4], **Md Shofiqul Islam**[1], **Padmanabhan Thirunavukkarasu**[6], **Mohammad Sohrab Hossain**[4] and **Alistair McEwan**[2,7]

[1] Bangladesh Health Professions Institute, Savar, Bangladesh
[2] School of Biomedical Engineering, University of Sydney, Sydney, New South Wales, Australia
[3] School of Human Movement and Nutrition Sciences, University of Queensland, Brisbane, Queensland, Australia
[4] Centre for the Rehabilitation of the Paralysed, Savar, Bangladesh
[5] Braintree Speciality Clinic, Chennai, India
[6] Madras Medical College, Government Institute of Rehabilitation Medicine, Chennai, India
[7] Current address: Cerebral Palsy Alliance, The University of Sydney, NSW 2006, Australia
[*] Author to whom any correspondence should be addressed.

E-mail: md.malam@connect.polyu.hk

Keywords: non-invasive electrical stimulation, transcutaneous spinal cord stimulation (tSCS), neuromodulation, neurological injury, rehabilitation

Supplementary material for this article is available online

Abstract

Objective. Transcutaneous spinal cord stimulation, a non-invasive spinal cord neuromodulation method holds tremendous promise and hope to restore functions in individuals with paralysis resulting from spinal cord injury (SCI), cerebral palsy, stroke and other neurological conditions. Yet, there are relatively few options for such stimulation devices compared to conventional stimulators commonly used for neuromuscular electrical stimulation, transcutaneous electrical nerve stimulation, and functional electrical stimulation, particularly for people with neurological conditions in the developing countries. *Approach.* In this report, we present OpenXstim, an open-source, two-channel programmable electrical stimulator developed to advance research in non-invasive muscle, nerve, or spinal cord stimulation treatments. *Main results.* OpenXstim can deliver current pulses up to 110 mA with a compliance voltage of 96 V per channel. In benchtop testing, we found that the stimulator successfully generates high frequency (9 kHz) burst stimulation, a mode commonly used for spinal cord neuromodulation. The stimulator was further tested in two individuals with SCI and showed preliminary indications of functional improvement. However, large controlled trials are needed to establish efficacy. Although special care was taken in the design of the stimulator to ensure user safety, users are strongly warned to handle the device with utmost caution, as it can generate high voltage and current that may cause adverse health effects if not used properly. *Significance.* This programmable, open-source stimulator offers tangible hope for improving the accessibility of non-invasive neuromodulation treatments for people with paralysis worldwide. The design and complete source-code of the stimulator are freely available online in a public repository: https://github.com/OpenMedTech-Lab/OpenXstim

1. Background

Transcutaneous spinal cord stimulation (tSCS) is an emerging non-invasive technique that has shown promising results in enhancing functional recovery across several neurological conditions, including spinal cord injury (SCI) (Tefertiller *et al* 2022, Moritz *et al* 2024, Lucas *et al* 2025), cerebral palsy (CP) (Hastings *et al* 2022, Sachdeva *et al* 2024), stroke (Moshonkina *et al* 2022, Kreydin *et al* 2024), and traumatic brain injury (TBI) (Qian *et al* 2020, Calderone *et al* 2024). By delivering electrical stimulation through the skin to the spinal cord, tSCS aims to modulate spinal neural circuits and enhance

sensorimotor function. Evidence suggests that tSCS can lead to significant improvements in movement, muscle strength, and overall functional outcomes, particularly when combined with conventional activity-based rehabilitation methods (Gopaul *et al* 2025, Suggitt *et al* 2025). For successful neuromodulation, a single rectangular pulse or burst of tSCS at motor-threshold elicits evoked potentials to the muscles through efferent synaptic pathways (Alam *et al* 2020, Gelenitis *et al* 2025). Previous studies have demonstrated that moderate-intensity tSCS applied over the T11-T12 vertebrae can depolarize posterior root and simultaneously elicit bilateral monosynaptic reflexes in the quadriceps, hamstrings, tibialis anterior, and triceps surae muscles (Sayenko *et al* 2015, Calvert *et al* 2019, Gordineer *et al* 2024). It was further demonstrated that monosynaptic posterior root reflexes in extensor and flexor muscles of thigh and leg can be elicited by stimulating L2-S1 spinal segments in upright standing position, and can be modulated during the execution of postural maneuvers (Hofstoetter *et al* 2018, Bryson *et al* 2023).

Tonic tSCS utilizes charge-balanced, symmetric, biphasic rectangular pulses at sub-threshold strengths to modulate the spinal cord circuits. The frequency of this tonic stimulation generally ranges from 5 to 100 Hz. Recent design includes modulated tSCS with a 5–10 kHz carrier frequency, which can successfully activate spinal circuits in human (Gerasimenko *et al* 2015, Shamantseva *et al* 2024), although some studies have found no significant benefit of using high carrier frequencies over conventional waveforms (Manson *et al* 2020, Dalrymple *et al* 2023). Recent studies have found that, in case of a disruption of the connection between the brain and the spinal cord, resulting from an injury or disease, motor tasks can be enabled by tSCS to the cervical and/or lumbosacral segments of the spinal cord (Martin 2021, Rahman *et al* 2022, Alam *et al* 2023). Modification of spasticity by tonic tSCS was also demonstrated in individuals with SCI (Hofstoetter *et al* 2020, Alashram *et al* 2021, Minassian *et al* 2024). In a recent study, it has also been demonstrated that tSCS can induce rhythmic activities of legs in robotic orthosis driven body-weight support system in upright position in people with complete SCI (Minassian *et al* 2016, Krenn *et al* 2023). Furthermore, repetitive gait training along with tSCS promotes long term functional recovery (Estes *et al* 2021, Comino-Suárez *et al* 2025).

Despite the growing success of tSCS in restoring functions in individuals with various neurological conditions, there are very few stimulators available that can deliver the specific stimulation parameters required—particularly high-frequency stimulation at 5–10 kHz. Furthermore, the ones that are available are expensive, bulky, and require careful laboratory setting and are not suitable for home or outdoor use. To address this a simple, low-cost, open source, programmable electrical stimulator was developed, and step-by-step prototyping of the stimulator was presented to allow others to make their own stimulator for tSCS therapy (Alam 2022). In the present report, an upgraded multichannel stimulator is presented which is capable of current pulse stimulation, crucial for more robust neuromodulation therapy. Several open-source electrical stimulators have been reported (Coelho-Magalhães *et al* 2022, Trout *et al* 2023). But, to the best of our knowledge, this is the first open-source electrical stimulator capable of high frequency burst stimulation. Special care has been given to minimize the complexity of the design by using commonly available components so that one can build one's own stimulator from anywhere in the world. In this report, we have also included two case studies in which participants demonstrated improvements in sensorimotor function following stimulation treatment using the OpenXstim stimulator.

2. Methods

2.1. Stimulator design

For easy prototyping, the electrical stimulator was designed using commonly available commercial off-the-shelf components. Functional block diagram of the stimulator is shown in figure 1. The stimulator contains 5 primary sections: (1) a power management unit build with a few DC–DC converters to serve necessary power for the stimulator, (2) a Microcontroller unit for easy programming that provides necessary parameters for the stimulation, (3) a control and display unit to vary the stimulation parameters and display the values, (4) a digital-to-analog converter (DAC) to generate voltage stimulation pulses, (5) a voltage-to-current converter unit to convert voltage pulses into appropriate current pulse. Operations of each of these are described in detail in the following sections.

2.2. Power management by DC–DC converters

The stimulator requires different voltages and power ratings for different sections. For instance, while the Microcontroller and display unit require only positive rail, the DAC and V/I circuit require both positive and negative rails to operate. Furthermore, due to the high skin impedance ($\sim$500 Ω at 1 kHz), transcutaneous stimulation requires high compliance voltage to be able to deliver necessary current through the skin. But, for safety and ease of use, these stimulators are commonly powered by a single NiCd/NiMH battery. The presented stimulator is powered by a single 9 V battery with relatively high ampere-hour ratings ($>$650 mAh) to be able to deliver necessary power. Figure 2 shows the power management circuit of the stimulator. The battery voltage is inverted to negative rail using a charge pump DC–DC converter

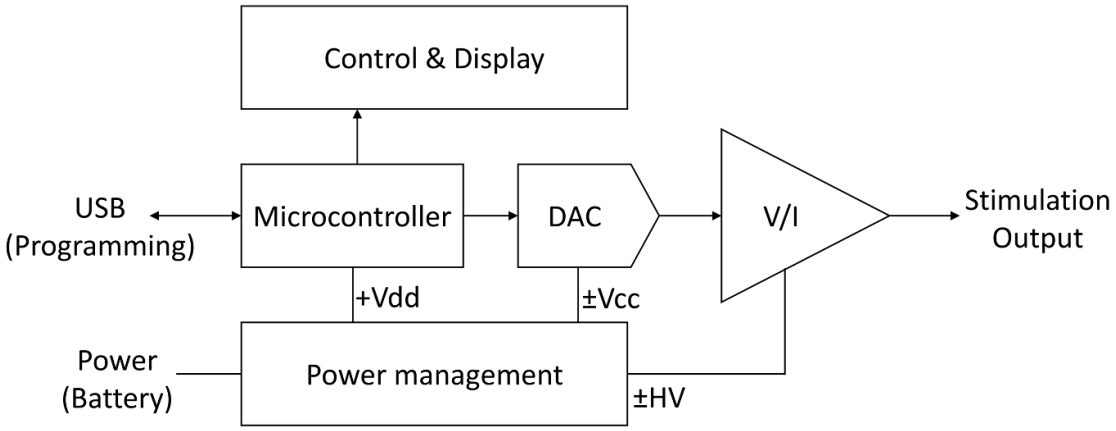

Figure 1. Block diagram of a transcutaneous electrical stimulator (OpenXstim) for non-invasive electrical stimulation. The stimulator has 5 major sections: a power management unit to serve necessary power for the stimulator, a Microcontroller unit for easy programming stimulation parameters, and a control & display unit to set and display the stimulation parameters, a digital-to-analog converter (DAC) to generate stimulation pulses, a voltage-to-current (V/I) converter unit to convert voltage pulses into appropriate current pulses.

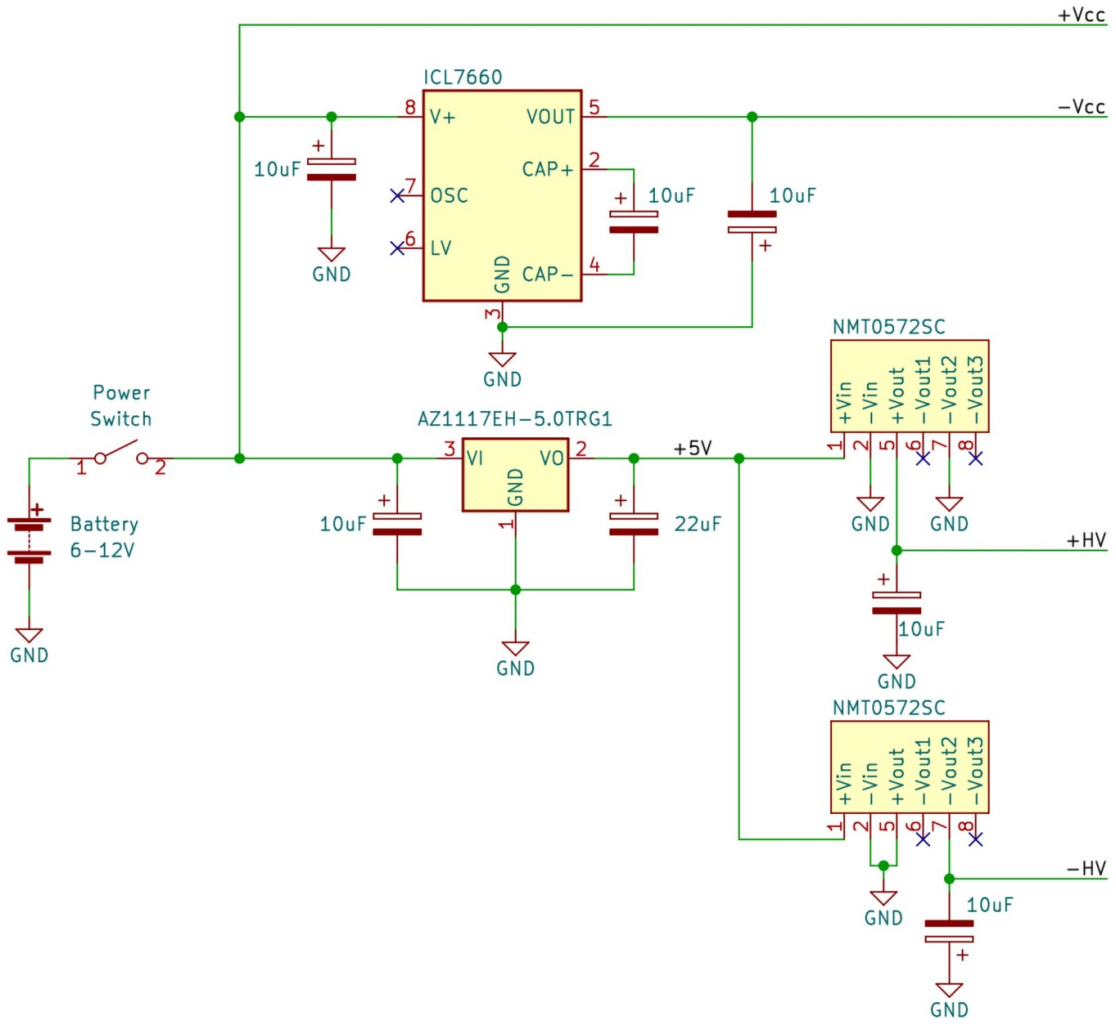

Figure 2. Schematic diagram of the power management circuit of OpenXstim stimulator. While the circuit allows any voltage between 6 to 12 volts to have stable operation, we recommend using a 9 V 650 mAh battery to power the stimulator.

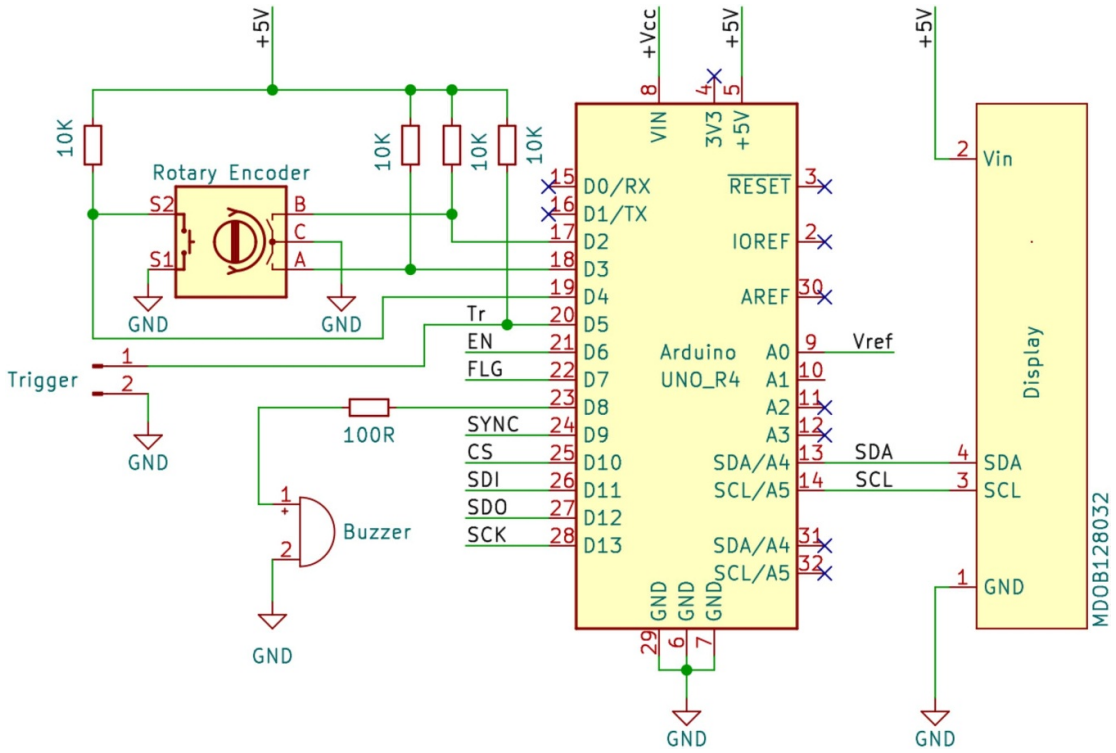

Figure 3. A rotary encoder and a display unit are wired to Arduino Uno Microcontroller board for quick change and display the stimulation parameters. A digital buzzer is also connected to the Microcontroller to allow audio notifications for different events as per programmed.

(ICL7660S) for the DAC circuit to be able to generate biphasic stimulation pulses. In parallel, to generate high voltage rails, two isolated DC–DC boost converters (NMT0572SC) are used. The boost converters are connected in such a manner to produce both high positive (+HV) and high negative (−HV) voltages. We used the -vout2 of NMT0572SC to get 48 volts rail for V/I converter circuit. A high-voltage 10 μF capacitor was used on each rail to store charge for high-current operation during the active cycle of the stimulation. Since the DC–DC boost converters can only operate with 5-volt input, we used another DC–DC voltage regulator (AZ117EH-5.0TRG1) to power both NMT0572SC. Necessary capacitors with appropriate voltage and charge ratings were used to regulate the voltage for each DC–DC converter chip. For details, please refer to appropriate datasheet provided by the chip manufacturer.

2.3. Set and display stimulation parameters (Microcontroller, Control and display unit)

The core of the stimulator is a very popular open-source Microcontroller board: Arduino Uno. While necessary firmware can be uploaded to the Microcontroller from a computer using a standard USB cable to run the stimulation program, a digital rotary encoder (PEC12R-4025F-S0024) was used to allow quick parameter changes. A rotary encoder typically uses a rotating disk with patterns and a magnetic sensor to produce pulses as the disk turns. Taking advantage of two interrupt pins of Arduino Uno (figure 3 shows the wiring diagram), the output signals of PEC12R-4025F-S0024 rotary encoder sends the microcontroller to specific interrupt service routine (ISR) to increase or decrease output current. This method ensures precise and efficient handling of the encoder's output by responding immediate pulse changes. The rotary encoder also includes a built-in press-switch function, which allows switching between current intensity and frequency adjustment modes. Pressing the knob activates a subroutine in the firmware (supplementary 1) that enables frequency control using the same rotary count mechanism. The stimulation parameters and other information are displayed to an OLED display (MDOB128032) connect via the I2C bus of the Microcontroller. We used SSD1306 display driver, developed by Adafruit for the OLED display. Figure 3 shows the complete wiring diagram of the PEC12R-4025F-S0024 rotary encoder and MDOB128032 display to the Microcontroller.

2.4. Biphasic pulse generation by DAC

To generate bipolar output voltage, a dual channel 12-bit Digital to Analogue Converter (AD5722) was used. The DAC is controlled through a standard 4-wire serial peripheral interface bus. Figure 4 shows the wiring diagram of AD5722 for Arduino Uno Microcontroller. A voltage divider made by two 1k

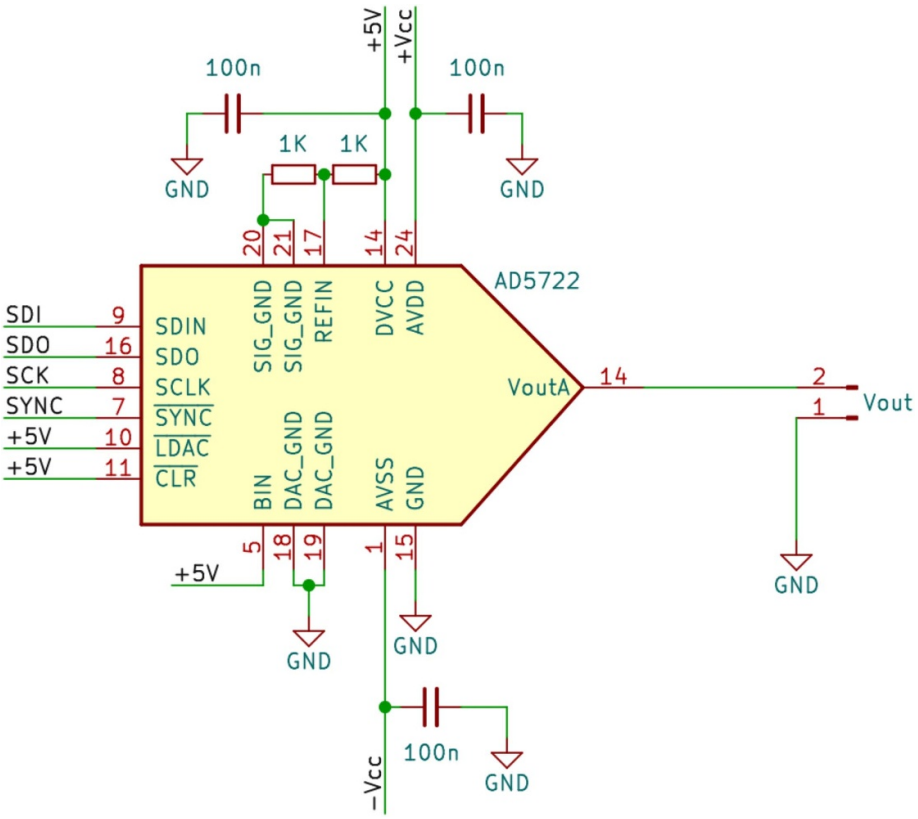

Figure 4. Schematic diagram of AD8722, a dual channel 12 bit digital-to-analog converter (DAC). For simplicity, only one channel is shown (VoutA).

resistors was used to supply the reference voltage. As mentioned in the power management section, the DAC is supplied with both positive and negative analogue power rails (±5 V) to allow it to generate bipolar voltage stimulation. For bipolar output range, the output voltage expression for AD5722 is shown below:

$$V_{\mathrm{OUT}} = V_{\mathrm{REF}} \times \mathrm{Gain}\frac{D}{2^N} - \frac{\mathrm{Gain} \times V_{\mathrm{REF}}}{2} \quad (1)$$

where:

D is the decimal equivalent of the value loaded to the DAC
N is the bit resolution (12)
V_{REF} is the reference voltage applied to the REFIN pin (2.5 volt)
Gain is the internal gain (set to 4 for ±5 V output span)

2.5. Generating current pulses by voltage-to-current (V/I) converter

The bipolar voltage output from each DAC channel is converted to constant current using an improved Howland current pump circuit (figure 5). A high-voltage (100 V), high-current (50 mA) operational amplifier (OPA454) was used to deliver the required high rating current pulses for the stimulator. Current pulses were generated by alternating the input voltage (V_{in}) of the improved Howland current pump circuit. This is done by programming the DAC to output alternating voltages at a stimulation frequency. We also used highly matched 25 kΩ (±0.1%) resistors array (ORNTA2502AT1) to convert the input voltage into a precise output current. In this V/I converter circuit, matched resistors are crucial for maintaining accuracy and stability. The op-amp in the circuit controls the current through the load based on the ratio of the resistors. A 50 Ω current control resistor (Rx) was used to set-up voltage-to-current ratio as shown in the following equation:

$$I_{\mathrm{OUT}} \approx \frac{V_{\mathrm{in}}}{\mathrm{Rx}} \quad (2)$$

where:

(R4 + Rx)/R2 = R3/R1;

Ideally, when both positive and negative feedback of the operational amplifier are balanced, an infinite output impedance is achieved. As a result, the output current is simply the ratio of the input voltage to the input impedance which is primarily determined by the current control resistor (Santos *et al* 2013).

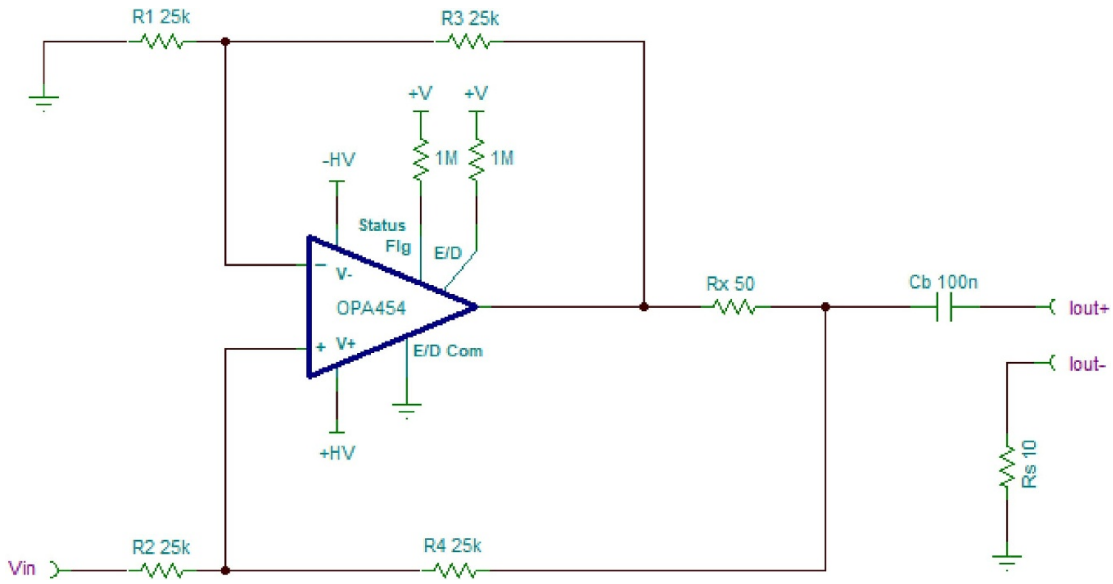

Figure 5. Improved Howland current pump using high-voltage high-current operational amplifier (OPA454) working as a precise voltage-to-current (*V*/*I*) converter circuit. A 25 kΩ quad matched resistor array (ORNTA2502AT1) is necessary to provide stable output current for the stimulator.

Two 1 MΩ pull-up resistors are also required for correct operation of the OPA454 operational amplifier. A 100 nF blocking capacitor is warranted for the protection of DC current to pass through the stimulation electrode in case the stimulator malfunctions. This is an important safety measure one should follow for electrical stimulation of biological tissues (Merrill *et al* 2005, van Dongen and Serdijn 2016). The stimulation current was also passed through a 10 Ω current sense resistor to allow continuous monitoring of the stimulation pulses.

2.6. Prototyping the stimulator

Step 1: Develop and assemble stimulator shield board

The complete schematics of the stimulator shield board was developed using an open-source electronic design automation (EDA) software (KiCAD 6.0). Gerber files were generated for prototyping the printed circuit board (PCB) of the stimulator shield board. A two-layer PCB was prototyped through a PCB manufacturer service (JLCPCB, Hong Kong SAR). All the components were sourced and assembled on the PCB through hand soldering. Figure 6(a) shows the 3D model of the assembled stimulator shield board. Standard male header pins were soldered on the bottom of the shield board to allow it to mount on the Microcontroller development board.

Step 2: Stack the stimulator shield on an Arduino Uno board and housing the assembled stimulator

The stimulator shield board was developed with the same footprint of an Arduino Uno development board so that it can easily be stacked on it (figure 6(b)). Arduino Uno is probably the most popular and widely available open-source Microcontroller board, allowing our stimulator to be taken up in most places around the world. Arduino Uno already has onboard female header pins allowing a shield board to be easily mounted on it.

The next step of prototyping is to build a case to house the stimulator to protect the electronics and the users from accidentally touching the components during its operation. We used a computer aided design software (SolidWorks, USA) to design the stimulator's case, knob, and switch. First, we extracted a 3D model of the stimulator board using EDA software (KiCAD 6.0, USA). The model was then imported into the assembly document, where we began designing the bottom part of the case by creating a new part. The base outline was sketched based on the board's dimensions; and then extruded to generate a 2 mm thick base. We then added the walls of the case by sketching an outline on the base followed by extrusion to desired height. Functional openings for ventilation and component connections were created. This process was repeated for all components, with each model saved and printed using PLA material on a 3D printer (Adventurer 3, Flashforge, China). Figure 6(c) shows an exploded view of the stimulator.

Step 3: Program the Stimulator

To program the Microcontroller, the Arduino Uno board was connected to a PC via a USB cable. After successfully selecting Arduino Uno board from the menu of Arduino IDE, the firmware was downloaded into the Microcontroller. The program flowchart

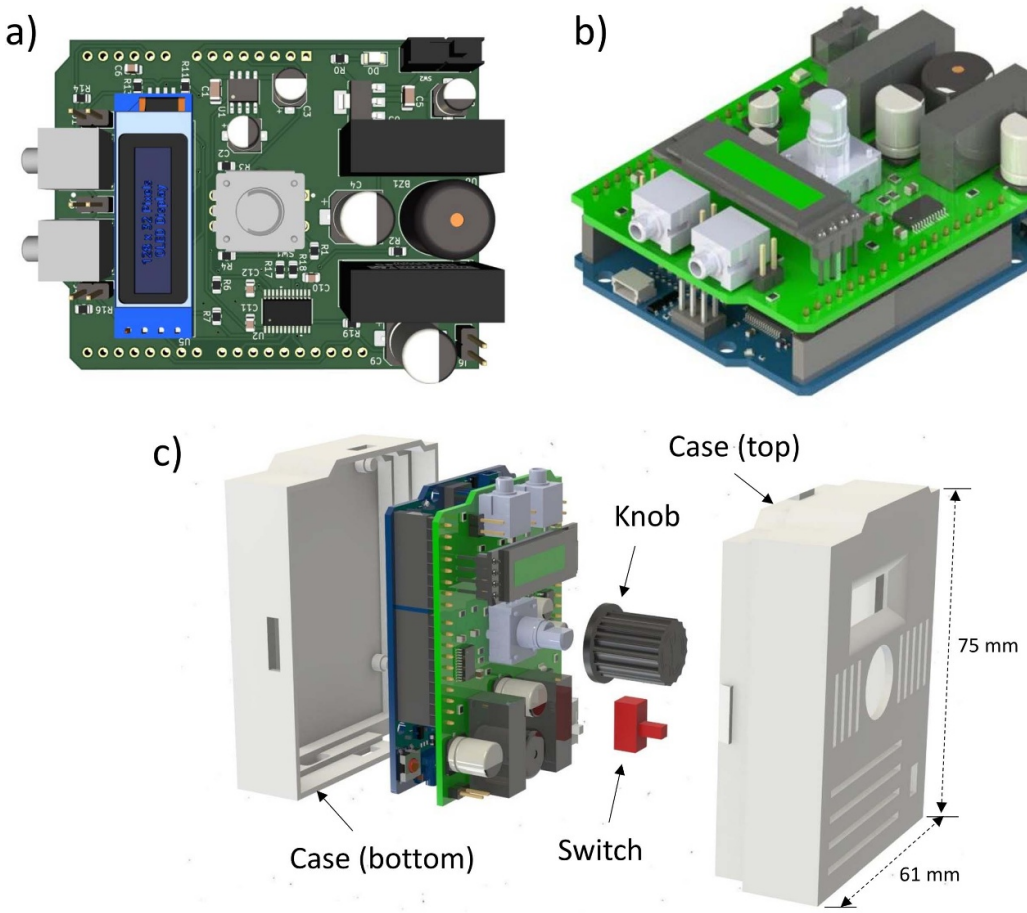

Figure 6. (a) 3D electronic design automation (EDA) model of assembled stimulator shield board. (b) Stimulator shield board stacked on an Arduino Uno Microcontroller development board through standard header pins. (c) Stimulator case, knob and switch printed using a 3D printer to house the stimulator board.

is shown in figure 7. After the start, stimulation parameters including stimulation frequency, pulse width, burst duration etc. are defined. Next, all the hardware connected to the Microcontroller are initialized by calling appropriate libraries. Then, in a loop N number of biphasic stimulation pulses are generated by writing the defined value to the DAC register. After this loop of stimulation (active burst burst), a delay (inter-burst delay calculated based on the defined stimulation frequency) was added to complete the stimulation cycle. The entire process runs again and again to repeat the stimulation indefinitely until it is powered off.

An ISR was also defined to allow the user quickly to change the stimulation intensity and frequency without re-programming the Microcontroller. Once the rotary encode is rotated, it initiates hardware interrupt of the Microcontroller which triggers the program to break the continuous main loop and jump into the ISR. In the ISR, the program increments or decrements the variable base on the data it reads from the rotary encoder. After that the program returns to the main loop, but now with the updated value of the variable which essentially reflects on the stimulation (an increased or decreased stimulation intensity).

The entire source code of the firmware is shared in the stimulator's GitHub repository as well as attached in supplementary 1.

2.7. Benchtop testing the stimulator

The stimulator tested on a benchtop setup. Figure 8 shows the experimental setup. The stimulator was powered by a 9 V battery using barrel adapter. The outputs were connected to two loads, one is 100 Ω resistor and the other is a Randles equivalent circuit of human skin (∼500 Ω impedance at 1 kHz) to test the functionality of the stimulator and emulate the expected operating conditions. A dual channel oscilloscope was used to monitor the voltage across the loads as well as to record the stimulator's output signal. Stimulation current was varied from 0–140 mA at 20 Hz stimulation (packed with 10 burst pulses at 9 kHz). Data from the oscilloscope were recorded and analyzed to assess the performance of the stimulator in terms of its current, waveform shape, and frequency.

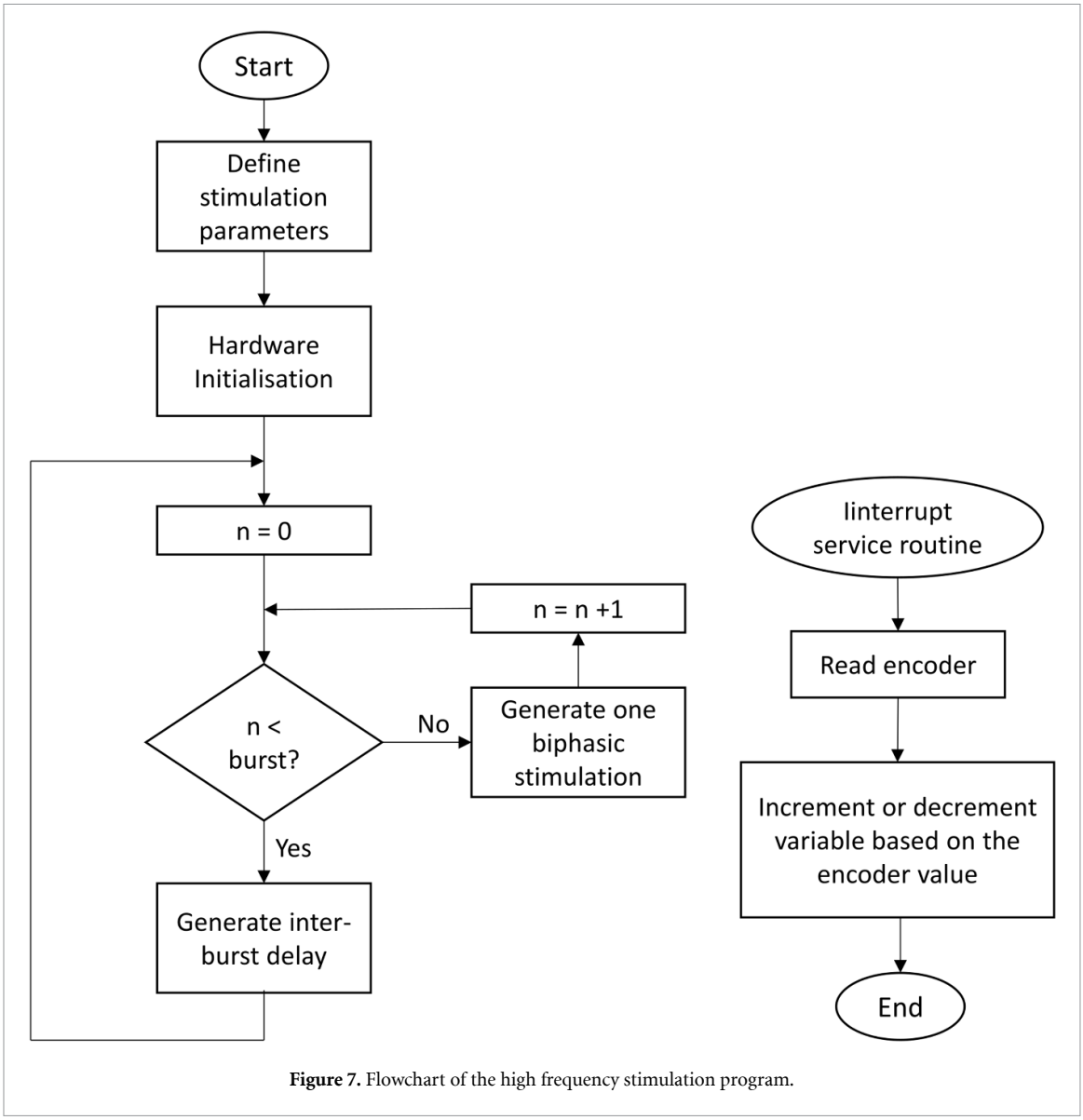

Figure 7. Flowchart of the high frequency stimulation program.

2.8. Clinical case studies

To test the stimulator, we conducted a series of clinical case studies involving individuals with chronic SCI (Trial registration No. ACTRN12625001081404). Eligible participants were required to be at least one-year post-injury, medically stable, and have previously completed a course of conventional physiotherapy without significant neurological improvement. Individuals with uncontrolled comorbidities, open wounds at stimulation sites, implanted electrical devices, or contraindications to electrical stimulation were excluded. The aim was to evaluate the device's ability to safely deliver tSCS in combination with conventional physiotherapy, assess participant comfort and tolerance, and observe any preliminary functional changes in a feasibility context. Two self-adhesive stimulation electrodes with a diameter of 3.2 cm (ValuTrode, Axelgaard Manufacturing Co. Ltd) were placed over the interspinous space between T11-T12 and L1-L2, and two internally connected 6.0 × 9.0 cm self-adhesive rectangular return electrodes (Guangzhou Jetta Electronic Medical Device Manufacturing Co. Ltd, China) placed above the iliac crests (Alam *et al* 2020). Before each stimulation session, the skin was checked to ensure it was free from irritation or wounds. Electrodes were placed with full adhesion and monitored throughout to maintain conductivity and prevent discomfort. These precautions helped minimize the risk of skin irritation or burns during stimulation. Figure 9 shows the electrodes placement and stimulation pattern used for the studies. To ensure safety, standard clinical monitoring was performed throughout each stimulation session to detect any signs of discomfort. During the initial sessions, stimulation was applied at lower intensities and for shorter durations, with gradual increases based on participant tolerance. The electrode sites were inspected regularly before and after each session for any signs of skin irritation or redness.

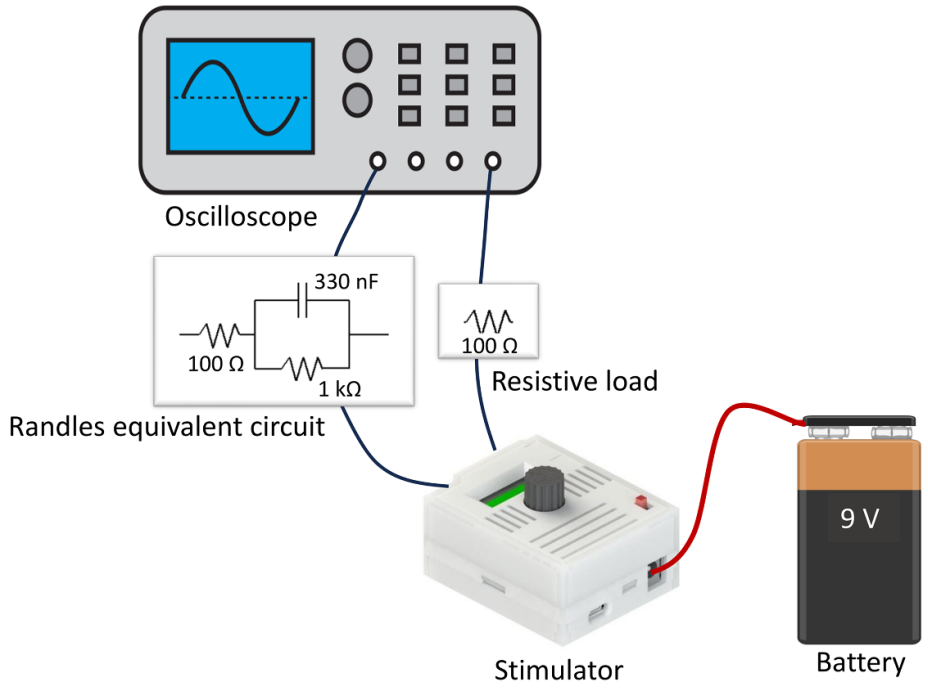

Figure 8. Benchtop setup for testing the functionality of the OpenXstim stimulator. The stimulator is powered by a 9 V battery. The output channels of the stimulator were connected to an oscilloscope through a resistive load (100 Ω) and Randles equivalent circuit (a 330 nF capacitor and a 1 kΩ resistor in parallel, connected in series with a 100 Ω resistor).

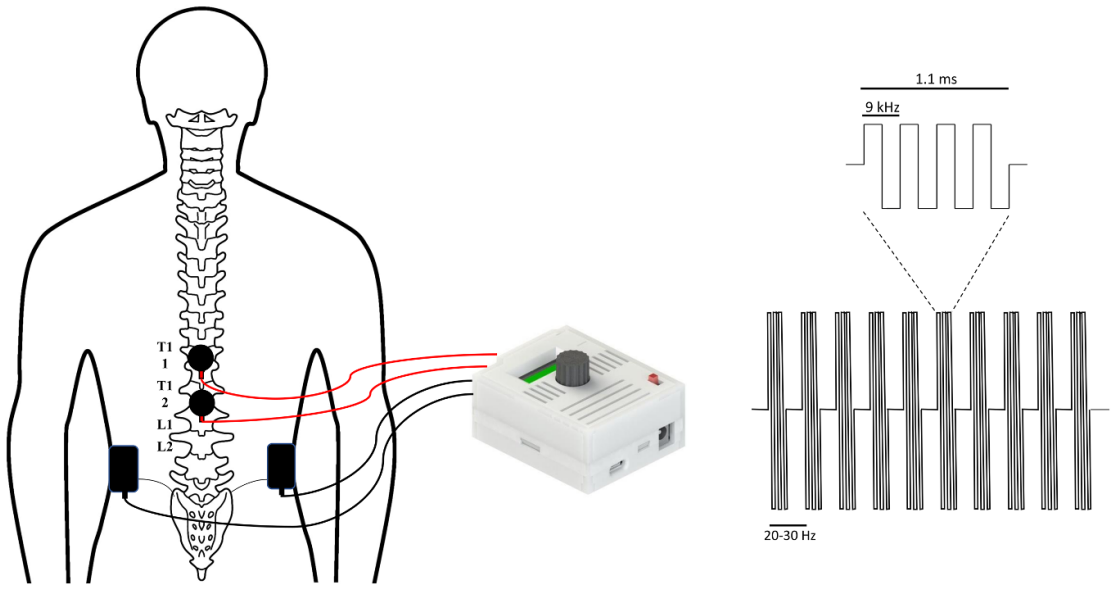

Figure 9. Electrodes placement of the OpenXstim stimulator (left) and high-frequency burst stimulation pattern (right) used for tSCS therapy.

Case 1:

The study participant was a 16 years old female who sustained a sensorimotor complete (ASIA-A) paraplegia following surgery for an arteriovenous malformation diagnosed at the thoracic 4 (T4) spinal cord. Post-surgery, she received regular physiotherapy upon being released from the hospital after her condition was stabilized. However, her sensorimotor condition did not change, and her paraplegia was considered permanent. Figure 10 shows the study procedure. The study was conducted in accordance with the Declaration of Helsinki and approved (Ref. CRP-BHPI/IRB/04/2025/1054) by the human research ethics subcommittee of the Centre for the Rehabilitation of the Paralyzed, Savar, Bangladesh.

At the beginning of the study, a certified physiotherapist assessed the study participant for her sensorimotor scores according to the International

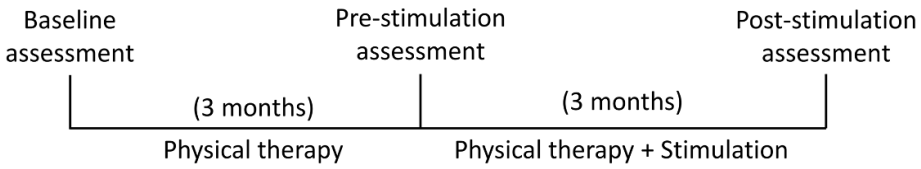

Figure 10. Study procedure. After baseline assessment of International Standards for Neurological Classification for SCI (ISNCSCI) for residual sensory and motor function, the study participant received conventional physical therapy for a period of 3 months followed by another ISNCSCI assessment. The study participant was then treated with transcutaneous spinal cord stimulation (tSCS) along with the same physical therapy for another 3 months. After the completion of this combinational treatment a final assessment was conducted.

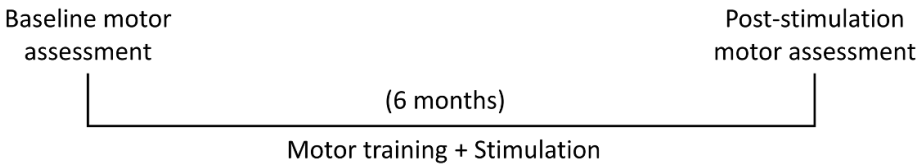

Figure 11. Study procedure. After baseline motor assessment (MAS), the study participant received a combinational treatment of motor training along with transcutaneous spinal cord stimulation (tSCS) for a period of 6 months. After the completion of this treatment a final motor assessment (MAS) was carried out.

Standards for Neurological Classification for SCI (ISNCSCI). The same physiotherapist also assessed her two more times: at 3 month and 6 month timepoints. During the first phase of treatment, the study participant received a conventional physiotherapy for about 35 min, 3 times a week for 3 months: first 15 min session was sitting balance practice (both static and dynamic condition), then 5 min rest and second 15 min session was standing and sit-to-stand practice with the assistance of the physiotherapist. After a thorough sensorimotor assessment (ISNCSCI), in the second phase of the study, the participant received the same physiotherapy but with stimulation tSCS at T11 and L1 spinal levels at 20 Hz, packed with 9 kHz biphasic pulses. The stimulation current was set to a current level that was comfortable to the study participant (40–60 mA) during the physiotherapy session. At the end of the study, the study participant was again assessed (ISNCSCI) for her sensorimotor changes by the same assessor.

Case 2:

A 43 years old female with no significant comorbidities sustained a traumatic SCI following a fall that resulted in a fracture of the T11 spinous process. A posterior spinal fusion from T10 to L1 was performed within 24 h. Post-surgery, she was diagnosed with both motor and sensory complete SCI (ASIA-A) paraplegia, which improved to T11 by discharge. Since her recovery, she had undergone functional electrical stimulation (FES) cycling 1-3 times per week and body-weight supported treadmill walking twice a day. At 2 years post-injury, the ISNCSCI assessment showed limited muscle function: the bilateral hip flexors were graded at 1/5, with very faint movement on the left side. The right knee extensors also showed minimal function, graded at 1/5. All other muscle groups tested were graded at 0/5, indicating no muscle activity in those areas. Figure 11 shows the study procedure. The study was conducted in accordance with the Declaration of Helsinki and was approved (Ref. IEC-MMC/Approval/04032024) by the Institutional Ethics Committee, Madras Medical College, Chennai, India.

At the beginning of the study, a certified physiotherapist assessed the study participant for her sitting function according to the Motor Assessment Scale (MAS). Same physiotherapist also assessed her after 6 month of stimulation assisted motor training. The stimulation intensity and frequency were adjusted according to the task to achieve the desired response. The study participant underwent training 3–5 d a week, focusing on tasks such as sit-to-stand (20 Hz, 30 mA biphasic stimulation), trunk dynamic balance in sitting (20 Hz, 50–70 mA biphasic stimulation), and body-weight supported gait training (30 Hz, 30 mA biphasic stimulation), with each session lasting 20–30 min. The study was approved (Ref. IEC-MMC/Approval/04032024) by the Institutional Ethics Committee, Madras Medical College, Chennai, India.

3. Results

3.1. OpenXstim: A light-weight versatile stimulator

OpenXstim is an open-source programmable current pulse stimulator capable of transcutaneous stimulation. Figure 12 shows the prototyped stimulator. The stimulator was lightweight (<100 gm), portable

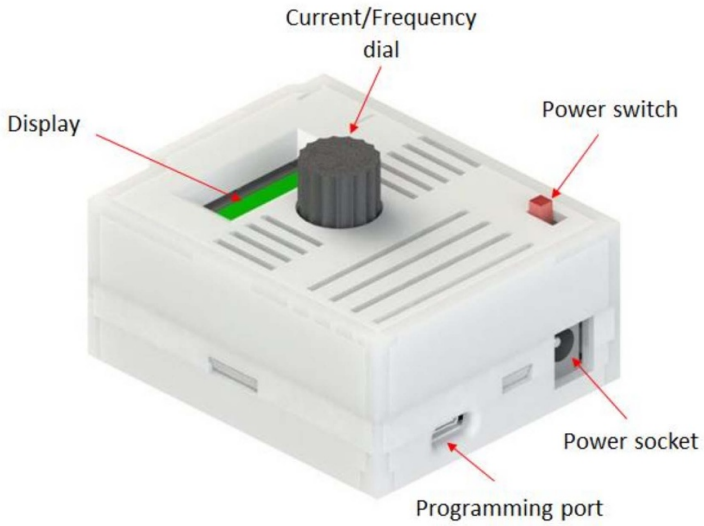

Figure 12. OpenXstim, open-source transcutaneous electrical stimulator. The stimulator can be powered by a 6–12 V battery with standard barrel jack. Power switch enables the output to deliver stimulation current. The current intensity and frequency are varied using the dial (black) in the center—mode can be selected by pressing the dial knob. The set value is dynamically displayed on the screen of the stimulator.

Table 1. Specifications of the OpenXstim transcutaneous electrical stimulator.

Channel count	2 channels
Mode of operation	Current pulse
Stimulation waveform	Monophasic/Biphasic (programmable)
Stimulation intensity	0–110 mA
Compliance voltage	Maximum 96 V (peak-to-peak)
Pulse duration	Minimum 50 μs (programmable)
Stimulation frequency	Maximum 9 kHz (programmable)
Power supply	6–12 V DC

(battery powered), and easy to use, with participants and clinicians finding it simple to transport and operate. The rotary knob control made to adjust the current and the frequency was straightforward, and the therapists reported no difficulties in using the device. The stimulator was compact enough to be carried and placed in the required treatment locations, and there were no issues with the electrode or cable during the study. The device performed reliably over the six-month usage period, demonstrating strong feasibility and usability. However, an improvement could be made with the battery design—having a built-in, rechargeable battery would eliminate the need for frequent replacements and enhance the overall user experience. Detailed specifications of the stimulator are listed in table 1.

3.2. OpenXstim can generate high frequency burst stimulation

In the present study, both channels of the stimulator were programmed to deliver high frequency burst pulses in-phase for transcutaneous electrical stimulation. The stimulator was tested on a benchtop setup; each channel of the stimulator connected to a load (see Methods section) for its functionality. Figure 13 illustrates the induced voltage across the load for 100 mA stimulation current. Ch 1 is the voltage across the Randles equivalent circuit whereas Ch 2 is the voltage across the resistive load. Both signals show successful biphasic burst stimulation at around 9 kHz.

The biphasic stimulation burst generated by the OpenXstim stimulator contains very short ($<$1 ns) inter-pulse interval due to the very fast operation of its DAC (see figure 13), a significant improvement from a commercial research stimulator (DS8R, Digitimer, United Kingdom) commonly used for transcutaneous stimulation where minimum inter-pulse interval is 1 μs. Furthermore, unlike many commercial electrical stimulators that uses multiplexed timesharing stimulation of multichannel stimulation (Valtin *et al* 2016), both stimulation channels of OpenXstim can stimulate simultaneous, providing greater flexibility of stimulation therapy.

The stimulator was also tested for its functionality of delivering required stimulation current at different intensities. Figure 14 shows the set vs measured stimulation currents across two loads. The results show excellent linear fits ($R^2 = 0.9987$ and 0.9997) of measured current values. However, the current does not appear to reach the set value, indicating a calibration offset. For the stimulation treatment, the current intensity was much lower than the maximum value.

Case 1: Restoration of somatosensory function using OpenXstim stimulator

Our study participant suffered a sensorimotor complete (ASIA-A) paralysis and received conventional physiotherapy followed by a combinational

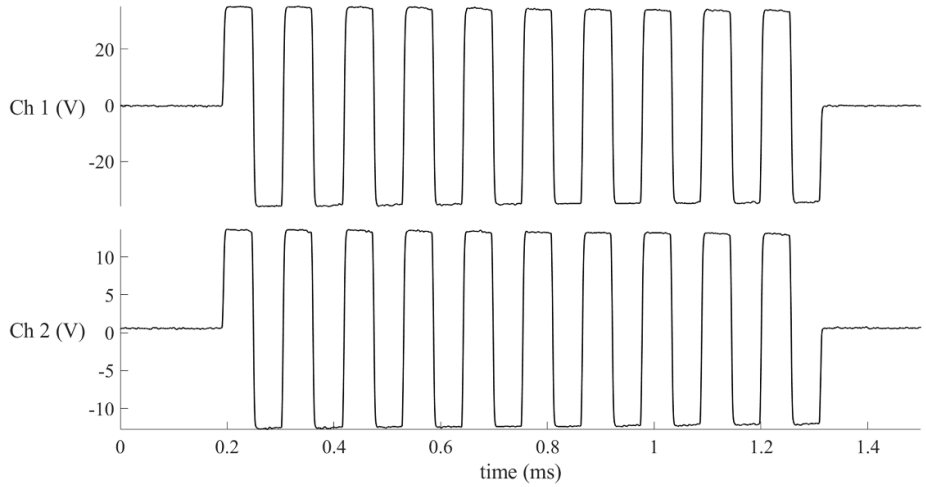

Figure 13. Induced voltage of 10 biphasic stimulation pulses at around 9 kHz burst stimulation across a Randles equivalent circuit (Ch 1) and a resistive load (Ch 2).

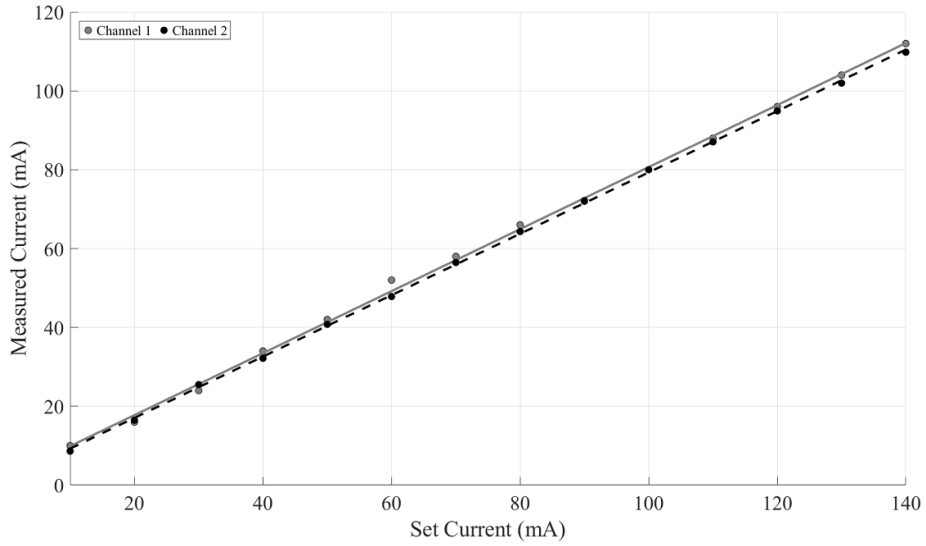

Figure 14. Set vs measured stimulation currents across loads. Blue line fits the data points measured for Channel 1 and black line fits the data points measured for Channel 2.

physiotherapy and tSCS. After 3 months of conventional physiotherapy (conservative management) without electrical stimulation, the ISNCSCI score remained the same as the baseline (motor and sensory complete ASIA-A). But after 3 months of physiotherapy with tSCS ASIA scale changed to ASIA-B (motor complete but sensory incomplete). Furthermore, the study participant got some sensory improvements as shown in figure 15. By the end of the study her sensory level for neurological injury changed from T4 to T5.

The tSCS therapy delivered by the OpenXstim was found to be well-tolerated, with preliminary indications of sensory improvement below the level of injury. The stimulation current was generally well-tolerated; however, due to the participant's young age and unfamiliarity with the intervention, initial nervousness was reported in response to the novel sensations induced by tSCS. Over time, with continuous support and reassurance from the caregiver and clinician, the participant gained confidence and became increasingly comfortable as the study progressed.

Case 2: Improvement of motor functions after tSCS therapy

After 6 months of motor training with tSCS therapy delivered by the OpenXstim stimulator, the study participant showed improvements in sitting balance with forward weight shifting, and the study participant is now able to reach forward with better

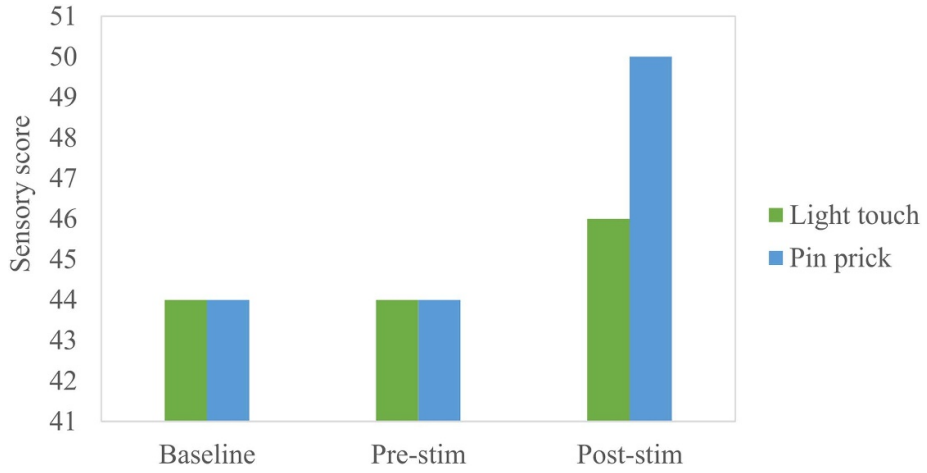

Figure 15. Total light touch and pin prick sensory scores according to the ISNCSCI at baseline, after 3 months conventional training (pre-stimulation) and 3 months conventional plus stimulation training (post-stimulation).

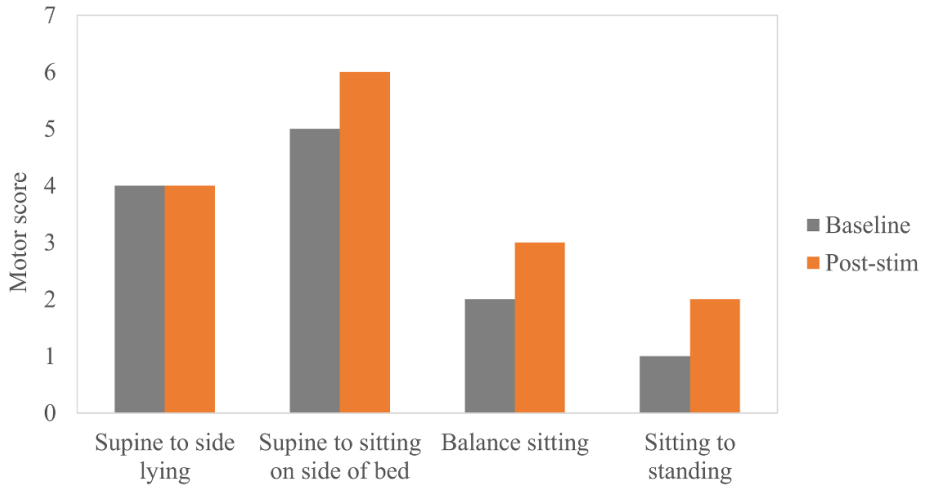

Figure 16. Baseline vs post-stimulation scores according to the Motor Assessment Scale (MAS) for different posture transitions.

core stability. Figure 16 shows changed in balance sitting and performance in postural transitions (supine to side lying, supine to sitting on the side of the bed and sitting to standing) before and after stimulation assisted motor training according to the MAS. Except supine to side lying, all other functions have improved after the stimulation training.

The tSCS was found to be feasible and safe, with early signs of improved core stability. The stimulation current was generally comfortable; however, when the battery charge depleted, it was not possible to lower the intensity before switching off the stimulator. This direct shutdown caused discomfort for the study participant, highlighting the importance of using high-rate battery that allows slowly reducing intensity prior to turning off the device.

4. Discussion

4.1. Clinical significance and the need for accessible neuromodulation devices

Each year, an estimated 250 000–500 000 new cases of SCI are reported globally (Nuechterlein *et al* 2023), often resulting in life-altering and debilitating conditions. Recent studies have highlighted the potentials of tSCS as an effective neuromodulation therapy not only for SCI rehabilitation (Hofstoetter and Minassian 2022, Rahman *et al* 2022) but also for a range of neurological conditions, including CP (Gad *et al* 2021, Hastings *et al* 2022), TBI (Qian *et al* 2020, Calderone *et al* 2024) and Stroke (Moon *et al* 2024, Zhang *et al* 2024). Despite its growing therapeutic promise, access to tSCS remains limited due to the high cost, bulkiness, and proprietary nature of most available stimulators. In this report, we present

Table 2. List of electrical stimulators used for non-invasive spinal cord stimulation (tSCS) therapy.

Name	Company	Approval	Channel	Power	Price
Biostim-5 (Grishin *et al* 2019)	Cosyma Inc.	N/A	5	Battery	N/A
NeoStim-5 (Parhizi *et al* 2021)		N/A	5	Battery	N/A
ARC_{EX} (Samejima *et al* 2022)	ONWARD Medical Inc	FDA	4	Battery	N/A
Stimulette r2x (Hofstoetter *et al* 2021)	Schuhfried Medizintechnik GmbH	N/A	2	Line	N/A
SCONE™ (Kreydin *et al* 2022)	SpineX Inc.	FDA Breakthrough	2	Battery	N/A
SCiP (Gad *et al* 2021)		Device	2	Battery	N/A
DS8R (Alam *et al* 2020)	Digitimer Ltd	N/A	1	Line	£8,335
OpenXstim	Present report	N/A	2	Battery	<$200

OpenXstim, a low-cost, open-source transcutaneous electrical stimulator designed to improve the accessibility and affordability of spinal cord stimulation—particularly in low- and middle-income countries (LMICs).

4.2. Bridging the gap: OpenXstim for global research equity

The overarching aim of this work is to enhance research capacity, particularly within low-resource settings, by offering an affordable and openly accessible transcutaneous electrical stimulation platform in line with the 2030 UN Sustainable Development Goals. Financial constraints and limited access to proprietary technologies are two major barriers that continue to hinder research and development in these regions, despite the presence of substantial technical expertise and scientific talent (Leal Filho *et al* 2022). By addressing these barriers, this work seeks to catalyze innovation and enable researchers—especially in LMICs—to design and conduct ethically approved studies using a device tailored to their specific needs. Since the presented stimulator is fully programmable and supports and supports a wide bandwidth of stimulation parameters, it can be easily configured to deliver standard protocols including neuromuscular electrical stimulation, transcutaneous electrical nerve stimulation, and FES, as well as experimental paradigms such as high-frequency tSCS. Table 2 shows the list of transcutaneous electrical stimulators used for non-invasive spinal cord stimulation therapy in people with neurological conditions.

4.3. Open-source commitment and design affordability

The presented stimulator (OpenXstim) provides an easy-accessible tool for non-invasive spinal cord stimulation to arguably for most communities around the world. The design schematics and source code for the stimulator are freely available online, allowing others to replicate or modify the device. All the design files, code and technical details can be freely downloaded from the OpenMedTech-Lab's GitHub repository (https://openmedtech-lab.github.io/). This open-source approach is a significant step toward making spinal cord stimulation therapy more affordable and accessible, particularly in resource-limited settings.

Components and modules used to build the OpenXstim stimulator are all listed in table 3. The total component cost of building the stimulator was only US$149.99; however, it can vary based on the market and supplies of the items. Additional costs should be considered for PCB prototyping and 3D printing of stimulator housing, which are significantly lower these days due to worldwide prototyping services. Reference prices and sources of all the components are also listed in table 3. Special care is given to choosing the most commonly available items so that anyone can build the stimulator anywhere in the world. One should, however, check with their local market and supplier for the availability of the components and modules. In case of unavailability, a similar module can be used, but care must be given to connect appropriate circuits and power.

4.4. Limitations and ensuring user safety

One of the primary limitations of this work is the small sample size, consisting of only two clinical case studies. The clinical case studies presented in this report are proof-of-concept feasibility tests, not designed to evaluate efficacy. While these cases offer preliminary insights into the feasibility of using OpenXstim for tSCS, they do not allow for generalization of outcomes or statistical significance. A controlled clinical study involving large sample size is necessary to evaluate the effectiveness of the spinal cord neuromodulation intervention delivered by OpenXstim across diverse populations and injury profiles.

An important limitation of this report is the use of different outcome assessment tools across the two case studies. While the ISNCSCI is the gold-standard measure for assessing sensory and motor recovery following SCI, the MAS was used in Case 2 to evaluate functional performance. The MAS

Table 3. Bill of materials (BOM) of OpenXstim with itemized cost in US dollars.

No.	Item name	Description	Unit price	Units	Subtotal
1	A1	Arduino UNO	20.64	1	20.64
2	BZ1	Buzzer	0.82	1	0.82
3	C1–C5	10 uF	0.24	5	1.2
4	C8	22 uF	0.75	1	0.75
5	C6, C7, C10–C14	100 n	0.24	7	1.68
6	D0	LED	0.27	1	0.27
7	IC1, IC2	OPA454	7.63	2	15.26
8	R0	270 R	0.16	1	0.16
9	R2	100 R	0.16	1	0.16
10	R1, R3, R4, R19	10 K	0.16	4	0.64
11	R6, R7, R9–R11, R13	1 M	0.16	6	0.96
12	R5, R8	ORNTA2502AT1	7.79	2	15.58
13	R12, R15	49R9	0.16	2	0.32
14	R14, R16	10 R	0.16	2	0.32
15	R17, R18	1 K	0.16	2	0.32
16	SW1	PEC12R-4025F-S0024	2.75	1	2.75
17	SW2	SW_SPDT	0.72	1	0.72
18	U1	ICL7660S	2.27	1	2.27
19	U2	AD5722AREZ	19.39	1	19.39
20	U3	AZ1117EH-5.0TRG1	0.75	1	0.75
21	U5	MDOB128032	12.61	1	12.61
22	U6, U8	NMT0572SC	26.21	2	52.42
		Total			**US$149.99**

was originally developed and validated for stroke rehabilitation; however, it has also been applied in individuals with SCI to evaluate sitting balance and functional transitions (Jørgensen *et al* 2011). Given that the participant in Case 2 primarily trained for sit-to-stand, dynamic trunk control, and gait tasks, MAS provided a sensitive measure of functional improvement that may not be captured by ISNCSCI motor scores (Tharu *et al* 2023). Nevertheless, the inconsistency in assessment tools limits the direct comparability between cases, and future studies should employ standardized and validated outcome measures specific to SCI rehabilitation.

Another key limitation is the absence of long-term safety data for the use of OpenXstim in chronic stimulation. Although short-term usage did not result in adverse effects in the current cases, prolonged or repeated exposure to electrical stimulation requires careful evaluation, especially given the potential for skin irritation, burns, or electrode-related complications. For additional safety, in our design, we used a DC blocking capacitor in each stimulation channel. This ensures stopping any prolonged constant voltage or current to be delivered to through the stimulation electrodes in the event of stimulator malfunction (van Dongen and Serdijn 2016). Additionally, to prevent risks such as uneven current distribution, burns, and electrode movement, it is essential to ensure that electrodes are securely and properly attached to the skin (Nussbaum *et al* 2017). Regularly inspect the gel for any signs of dryness or loss of adhesion, especially at the edges, and reapply as needed to maintain consistent contact. This helps to ensure proper conductivity and prevent the gel from lifting, which can lead to increased current density and other safety hazards.

In both case studies, managing electrical currents to prevent discomfort highlights the importance of controlling the intensity of stimulation. An additional feature that could be implemented to address this issue is the integration of current ramp-up/ramp-down functionality, a standard feature in many electrical stimulation systems (Nussbaum *et al* 2017). This feature gradually increases or decreases the electrical current, allowing for a smoother transition in muscle activation and preventing abrupt changes that could cause discomfort or injury. Ramping up the current gradually ensures that the muscles and tissues can adapt to the stimulation, particularly in sensitive individuals or during long-term usage. Similarly, ramping down the current allows for a safe reduction in intensity, which can help prevent sudden muscle release, thus improving safety and comfort throughout the therapy.

The stimulator's operability was also assessed during 30 min of continuous use, corresponding to the typical therapeutic session duration. Moderate heating was observed in the 5.0 V linear regulator (AZ117EH-5.0TRG1) and minimal heating in the DC–DC boost converter (NMT0572SC), indicating acceptable thermal performance. Future versions may

eliminate the linear regulator by using a regulated 5 V power source to improve efficiency and reduce heat buildup.

4.5. Future enhancements and expanded applications

The current OpenXstim firmware does not include real-time impedance monitoring, which is a standard feature in many clinical-grade stimulation devices. Continuous impedance monitoring is crucial for ensuring consistent and safe electrical delivery, especially in dynamic environments where electrode-skin contact may fluctuate due to movement, sweating, or drying of conductive gel (Vargas Luna *et al* 2015). Although our design utilizes a constant current source that dynamically adjusts its output current based on the variable load, the absence of real-time impedance monitoring may increase the risk of uneven current distribution, discomfort, or localized skin heating. Integrating impedance monitoring would not only enhance safety but also improve the precision of stimulation delivery and help prevent unintended fluctuations in current during therapy sessions. Our hardware design already includes circuitry—such as current sensing resistor and analog-to-digital converter—that enables load impedance measurement (see supplementary 1). However, this functionality has not yet been implemented in the firmware. Incorporating impedance monitoring into the firmware should be prioritized in future iterations of the device.

The calibration offset of the stimulation current is primarily due to small mismatches in the resistor network of the improved Howland current pump circuit. Despite using high-precision matched resistors, these mismatches—along with the influence of the current control resistor and the finite open-loop gain of the operational amplifier—can reduce output impedance and introduce load-dependent variations, especially at higher stimulation intensities (Ghorbani and Nahvi 2019). Future improvements may include tighter tolerance components and firmware-based closed-loop calibration to enhance accuracy and linearity.

Although the stimulator includes a power switch that can disconnect it is power anytime, adding an additional emergency stop switch would be beneficiary for the user. Additional features, such as wireless control and signal monitoring, can be easily incorporated to enhance the functionality and usability of the stimulator. Since the stimulator is an Arduino Uno shield, using an Uno board with wireless capabilities such as Minima or WiFi would allow it to function as a wireless stimulator. This modification would enable its use in extended applications, such as brain-computer interface control or electronic bypass of SCI, as we demonstrated previously (Alam *et al* 2014, Li *et al* 2014, McGeady *et al* 2022).

5. Conclusion

OpenXstim was designed using commercially available components to ensure global accessibility and ease of replication. Bench testing confirmed the device's ability to deliver reliable high frequency burst stimulation, while preliminary clinical case studies demonstrated its potential to improve sensory and motor function in individuals with chronic paralysis. OpenXstim addresses a critical gap in the availability of accessible neuromodulation technologies—particularly for use in low-resource settings. Its open-source design, including hardware schematics, firmware, and documentation, is freely available (https://github.com/OpenMedTech-Lab/OpenXstim) to support reproducibility and customization. OpenXstim represents a promising step toward democratizing spinal cord stimulation therapy and expanding global research capacity in neuromuscular rehabilitation.

Data availability statement

Design source files and additional documentation related to the OpenXstim stimulator are available in the online public repository: https://github.com/OpenMedTech-Lab/OpenXstim

Technical data set of OpenXstim v1.0 available at https://doi.org/10.1088/1741-2552/ae20c2/data1.

Acknowledgment

We sincerely thank the study participants for their time, valuable feedback, and contribution to the evaluation of the OpenXstim stimulator.

Conflict of interest

The authors declare no competing interests.

Funding

The authors did not receive any funding for this work.

Authors' contributions

M.A. wrote the main manuscript text with parts from V.N., M.A.R. and V.A. N.N., F.T. and M.S.I helped with the case studies. P.T. and M.S.H. examined and validated the clinical data. A.M. revised and corrected the main manuscript and provided inputs to improve the manuscript. All authors reviewed the final manuscript.

Consent for publication

Informed consent for publication of anonymized data and results was obtained from all the study participants.

Disclaimers

The stimulator design is provided as-is and, despite careful development and extensive testing, no warranties are offered regarding its performance or safety. The authors cannot be held liable for any accidents or misuse of the stimulator.

Ethics approval and consent to participate

The studies involving human participants were conducted in accordance with the ethical standards and with the 1964 Helsinki Declaration and its later amendments. Ethical approvals were obtained for both case studies.

Users' safety notes

- The design is intended exclusively for research and educational purposes.
- The stimulator has not been approved for use on humans or animals without prior authorization from a relevant ethics committee, such as an Institutional Review Board.
- The stimulator can produce high voltage. It must never be positioned across the chest, head, or in close proximity to the heart.
- The stimulator should never be powered through an external adapter, USB, or any other power source while in use or when connected to the body.
- Stimulation electrodes should be securely attached to the skin, and the gel remains intact to prevent uneven current distribution, and the risk of skin irritation or burns.

License

ORCID iDs

Monzurul Alam 0000-0003-0987-1999
Md Shofiqul Islam 0000-0001-8085-7976
Mohammad Sohrab Hossain 0000-0002-8452-1641
Alistair McEwan 0000-0001-7597-6372

References

Alam M 2022 An easy-to-build transcutaneous electrical stimulator for spinal cord stimulation therapy

Alam M, Chen X, Zhang Z, Li Y and He J 2014 A brain-machine-muscle interface for restoring hindlimb locomotion after complete spinal transection in rats *PLoS One* **9** e103764

Alam M, Ling Y T, Rahman M A, Wong A Y L, Zhong H, Edgerton V R and Zheng Y-P 2023 Restoration of over-ground walking via non-invasive neuromodulation therapy: a single-case study *J. Clin. Med.* **12** 7362

Alam M, Ling Y T, Wong A Y L, Zhong H, Edgerton V R and Zheng Y-P 2020 Reversing 21 years of chronic paralysis via non-invasive spinal cord neuromodulation: a case study *Ann. Clin. Transl. Neurol.* **7** 829–38

Alashram A R *et al* 2021 Transcutaneous spinal cord stimulation effects on spasticity in patients with spinal cord injury: a systematic review *J. Spinal Cord Med.* **46** 1–8

Bryson N, Lombardi L, Hawthorn R, Fei J, Keesey R, Peiffer J D and Seáñez I 2023 Enhanced selectivity of transcutaneous spinal cord stimulation by multielectrode configuration *J. Neural Eng.* **20** 046015

Calderone A, Cardile D, Gangemi A, De Luca R, Quartarone A, Corallo F and Calabrò R S 2024 Traumatic brain injury and neuromodulation techniques in rehabilitation: a scoping review *Biomedicines* **12** 438

Calvert J S, Manson G A, Grahn P J and Sayenko D G 2019 Preferential activation of spinal sensorimotor networks via lateralized transcutaneous spinal stimulation in neurologically intact humans *J. Neurophysiol.* **122** 2111–8

Coelho-Magalhães T, Fachin-Martins E, Silva A, Azevedo Coste C and Resende-Martins H 2022 Development of a high-power capacity open source electrical stimulation system to enhance research into FES-assisted devices: validation of FES cycling *Sensors* **22** 531

Comino-Suárez N, Moreno J C, Megía-García Á, Del-ama A J, Serrano-Muñoz D, Avendaño-Coy J, Gil-Agudo Á, Alcobendas-Maestro M, López-López E and Gómez-Soriano J 2025 Transcutaneous spinal cord stimulation combined with robotic-assisted body weight-supported treadmill training enhances motor score and gait recovery in incomplete spinal cord injury: a double-blind randomized controlled clinical trial *J. Neuroeng. Rehabil.* **22** 15

Dalrymple A N, Hooper C A, Kuriakose M G, Capogrosso M and Weber D J 2023 Using a high-frequency carrier does not improve comfort of transcutaneous spinal cord stimulation *J. Neural Eng.* **20** 016016

Estes S, Zarkou A, Hope J M, Suri C and Field-Fote E C 2021 Combined transcutaneous spinal stimulation and locomotor training to improve walking function and reduce spasticity in subacute spinal cord injury: a randomized study of clinical feasibility and efficacy *J. Clin. Med.* **10** 1167

Gad P, Hastings S, Zhong H, Seth G, Kandhari S and Edgerton V R 2021 Transcutaneous spinal neuromodulation reorganizes neural networks in patients with cerebral palsy *Neurotherapeutics* **18** 1953–62

Gelenitis K *et al* 2025 Non-invasive transcutaneous spinal cord stimulation programming recommendations for the treatment of upper extremity impairment in tetraplegia *Neuromodulation* **28** 162–73

Gerasimenko Y, Gorodnichev R, Moshonkina T, Sayenko D, Gad P and Reggie Edgerton V 2015 Transcutaneous electrical spinal-cord stimulation in humans *Ann. Phys. Rehabil. Med.* **58** 225–31

Ghorbani R and Nahvi M 2019 Analysis of performance of Howland AC current source for electrical impedance spectro-tomography *Sens. Imaging* **20** 28

Gopaul U, Bayley M T and Kalsi-Ryan S 2025 Combined activity-based therapy and cervical spinal cord stimulation: active ingredients, targets and mechanisms of actions to optimize neurorestoration of upper limb function after cervical spinal cord injury *Physiother. Res. Int.* **30** e70036

Gordineer E A, Stokic D S and Krenn M J 2024 Distinguishing reflex from non-reflex responses elicited by transcutaneous spinal stimulation targeting the lumbosacral cord in healthy individuals *Exp. Brain Res.* **242** 959–70

Grishin A A, Moshonkina T R, Bobrova E V and Gerasimenko Y P 2019 A device for the rehabilitation therapy of patients with motor pathology using mechanotherapy, transcutaneous

electrical stimulation of the spinal cord, and biological feedback *Biomed. Eng.* **53** 227–30
Hastings S, Zhong H, Feinstein R, Zelczer G, Mitrovich C, Gad P and Edgerton V R 2022 A pilot study combining noninvasive spinal neuromodulation and activity-based neurorehabilitation therapy in children with cerebral palsy *Nat. Commun.* **13** 5660
Hofstoetter U S, Freundl B, Binder H and Minassian K 2018 Common neural structures activated by epidural and transcutaneous lumbar spinal cord stimulation: elicitation of posterior root-muscle reflexes *PLoS One* **13** e0192013
Hofstoetter U S, Freundl B, Danner S M, Krenn M J, Mayr W, Binder H and Minassian K 2020 Transcutaneous spinal cord stimulation induces temporary attenuation of spasticity in individuals with spinal cord injury *J. Neurotrauma* **37** 481–93
Hofstoetter U S, Freundl B, Lackner P and Binder H 2021 Transcutaneous spinal cord stimulation enhances walking performance and reduces spasticity in individuals with multiple sclerosis *Brain Sci.* **11** 472
Hofstoetter U S and Minassian K 2022 Transcutaneous spinal cord stimulation: advances in an emerging non-invasive strategy for neuromodulation *J. Clin. Med.* **11** 3836
Jørgensen V, Elfving B and Opheim A 2011 Assessment of unsupported sitting in patients with spinal cord injury *Spinal Cord* **49** 838–43
Krenn M J, White J M, Stokic D S and Tansey K E 2023 Neuromodulation with transcutaneous spinal stimulation reveals different groups of motor profiles during robot-guided stepping in humans with incomplete spinal cord injury *Exp. Brain Res.* **241** 365–82
Kreydin E I *et al* 2024 A pilot study of the effect of transcutaneous spinal cord stimulation on micturition-related brain activity and lower urinary tract symptoms after stroke *J. Urol.* **211** 294–304
Kreydin E, Zhong H, Lavrov I, Edgerton V R and Gad P 2022 The effect of non-invasive spinal cord stimulation on anorectal function in individuals with spinal cord injury: a case series *Front. Neurosci.* **16** 816106
Leal Filho W *et al* 2022 An assessment of requirements in investments, new technologies, and infrastructures to achieve the SDGs *Environ. Sci. Eur.* **34** 58
Li Y, Alam M, Guo S, Ting K H and He J 2014 Electronic bypass of spinal lesions: activation of lower motor neurons directly driven by cortical neural signals *J. Neuroeng. Rehabil.* **11** 107
Lucas K *et al* 2025 Non-invasive spinal neuromodulation enables stepping in children with complete spinal cord injury *Brain***148** 3290–99
Manson G A, Calvert J S, Ling J, Tychhon B, Ali A and Sayenko D G 2020 The relationship between maximum tolerance and motor activation during transcutaneous spinal stimulation is unaffected by the carrier frequency or vibration *Physiol. Rep.* **8** e14397
Martin R 2021 Utility and feasibility of transcutaneous spinal cord stimulation for patients with incomplete SCI in therapeutic settings: a review of topic *Front. Rehabil. Sci.* **2** 724003
McGeady C, Vučković A, Singh Tharu N, Zheng Y-P and Alam M 2022 Brain-computer interface priming for cervical transcutaneous spinal cord stimulation therapy: an exploratory case study *Front. Rehabil. Sci.* **3** 896766
Merrill D R, Bikson M and Jefferys J G R 2005 Electrical stimulation of excitable tissue: design of efficacious and safe protocols *J. Neurosci. Methods* **141** 171–98
Minassian K, Freundl B, Lackner P and Hofstoetter U S 2024 Transcutaneous spinal cord stimulation neuromodulates pre- and postsynaptic inhibition in the control of spinal spasticity *Cell Rep. Med.* **5** 101805
Minassian K, Hofstoetter U S, Danner S M, Mayr W, Bruce J A, McKay W B and Tansey K E 2016 Spinal rhythm generation by step-induced feedback and transcutaneous posterior root stimulation in complete spinal cord-injured individuals *Neurorehabil. Neural Repair.* **30** 233–43
Moon Y *et al* 2024 Noninvasive spinal stimulation improves walking in chronic stroke survivors: a proof-of-concept case series *Biomed. Eng. Online* **23** 38
Moritz C *et al* 2024 Non-invasive spinal cord electrical stimulation for arm and hand function in chronic tetraplegia: a safety and efficacy trial *Nat. Med.* **30** 1276–83
Moshonkina T R, Zharova E, Ananev S, Shandybina N, Vershinina E, Lyakhovetskii V, Grishin A, Shlyakhto E and Gerasimenko Y 2022 A new technology for recovery of locomotion in patients after a stroke *Dokl. Biochem. Biophys.* **507** 353–6
Nuechterlein A, Feng L, Yehia A and Illes J 2023 Strengths, gaps, and future directions on the landscape of ethics-related research for spinal cord injury *Spinal Cord* **61** 477–82
Nussbaum E L, Houghton P, Anthony J, Rennie S, Shay B L and Hoens A M 2017 Neuromuscular electrical stimulation for treatment of muscle impairment: critical review and recommendations for clinical practice *Physiother. Can.* **69** 1–76
Parhizi B, Barss T S and Mushahwar V K 2021 Simultaneous cervical and lumbar spinal cord stimulation induces facilitation of both spinal and corticospinal circuitry in humans *Front. Neurosci.* **15** 615103
Qian Q *et al* 2020 Restoration of arm and hand functions via noninvasive cervical cord neuromodulation after traumatic brain injury: a case study *Brain Injury* **34** 1–10
Rahman M A, Tharu N S, Gustin S M, Zheng Y-P and Alam M 2022 Trans-spinal electrical stimulation therapy for functional rehabilitation after spinal cord injury: review *J. Clin. Med.* **11** 1550
Sachdeva R, Girshin K, Shirkhani Y and Gad P 2024 Beyond pediatrics: noninvasive spinal neuromodulation improves motor function in an adult with cerebral palsy *Bioelectron. Med.* **10** 1
Samejima S, Caskey C D, Inanici F, Shrivastav S R, Brighton L N, Pradarelli J, Martinez V, Steele K M, Saigal R and Moritz C T 2022 Multisite transcutaneous spinal stimulation for walking and autonomic recovery in motor-incomplete tetraplegia: a single-subject design *Phys. Ther.* **102** pzab228
Santos S, Schlebusch T and Leonhardt S 2013 Simulation of a current source with a Cole-Cole load for multi-frequency electrical impedance tomography *Annual Int. Conf. IEEE Engineering in Medicine and Biology Society* pp 6445–8
Sayenko D G, Atkinson D A, Dy C J, Gurley K M, Smith V L, Angeli C, Harkema S J, Edgerton V R and Gerasimenko Y P 2015 Spinal segment-specific transcutaneous stimulation differentially shapes activation pattern among motor pools in humans *J. Appl. Physiol.* **118** 1364–74
Shamantseva N, Timofeeva O, Semenova V, Andreeva I and Moshonkina T 2024 Transcutaneous spinal cord stimulation modulates quiet standing in healthy adults: stimulation site and cognitive style matter *Front. Neurosci.* **18** 1467182
Suggitt J, Symonds J and D'Amico J M 2025 Safety and effectiveness of multisite transcutaneous spinal cord stimulation combined with activity-based therapy when delivered in a community rehabilitation setting: a real-world pilot studySafety and effectiveness of multisite transcutaneous spinal cord stimulation combined with activity-based therapy when delivered in a community rehabilitation setting: a real-world pilot study Neuromodulation **28** 1144–56
Tefertiller C, Rozwod M, VandeGriend E, Bartelt P, Sevigny M and Smith AC 2022 Transcutaneous electrical spinal cord

stimulation to promote recovery in chronic spinal cord injury *Front. Rehabil. Sci.* **2** 740307

Tharu N S, Alam M, Ling Y T, Wong A Y and Zheng Y-P 2023 Combined transcutaneous electrical spinal cord stimulation and task-specific rehabilitation improves trunk and sitting functions in people with chronic tetraplegia *Biomedicines* **11** 34

Trout M A, Harrison A T, Brinton M R and George J A 2023 A portable, programmable, multichannel stimulator with high compliance voltage for noninvasive neural stimulation of motor and sensory nerves in humans *Sci. Rep.* **13** 3469

Valtin M, Kociemba K, Behling C, Kuberski B, Becker S and Schauer T 2016 RehaMovePro: a versatile mobile stimulation system for transcutaneous FES applications *Eur. J. Trans. Myol.* **26** 6076

van Dongen M N and Serdijn W A 2016 Does a coupling capacitor enhance the charge balance during neural stimulation? An empirical study *Med. Biol. Eng. Comput.* **54** 93–101

Vargas Luna J L, Krenn M, Cortés Ramírez J A and Mayr W 2015 Dynamic impedance model of the skin-electrode interface for transcutaneous electrical stimulation *PLoS One* **10** e0125609

Zhang J, Wang M, Alam M, Zheng Y-P, Ye F and Hu X 2024 Effects of non-invasive cervical spinal cord neuromodulation by trans-spinal electrical stimulation on cortico-muscular descending patterns in upper extremity of chronic stroke *Front. Bioeng. Biotechnol.* **12** 1372158